

MONOLYTHIC METHOD FOR THE SOLUTION OF THE FLUID-STRUCTURE INTERACTION PROBLEM

Julio Marti^a and Sergio Idelsohn^b

^a*International Center for Computational Method in Engineering (CIMEC), Universidad Nacional del Litoral and CONICET, Guemes 3450, Santa Fe, Argentina, jmarti@ceride.gov.ar,
<http://www.cimec.org.ar/~jmarti>*

^b*International Center for Numerical Methods in Engineering (CIMNE), Universidad Politécnica de Cataluña, Campus Norte UPC, 08034 Barcelona, Spain,*

Keywords: Lagrangian formulation, fluid-structure, particle finite element method.

Abstract. We propose a Lagrangian framework for modelling fluid-structure interaction (FSI) problems with free surfaces flows. The model is based on a Lagrangian approach for describing the fluid and structural dynamics. Our approach allows to treat the whole FSI domain as a single entity and describes its behaviour by a single set of momentum and continuity equations and which is solved using a single numerical method. This work uses the Particle Finite Element Method (PFEM) to solve the resulting differential equations. The PFEM is an effective technique for modelling complex interactions between floating and submerged bodies and free surface flows, accounting for splashing of waves, large motions of the bodies and frictional contact conditions. Examples are presented based on the model including free surfaces flows and breaking waves impacting over elastics structures.

1 INTRODUCTION

Historically, two fundamental frameworks to describe the relevant kinematics have dominated continuum mechanics research and applications. Firstly, one can follow the material in time and describe motion and deformation by registration of the successive spatial positions that each physical 'particle' occupies. This approach is commonly known as the Lagrangian description, and it is primarily used by the solid mechanics community. Secondly, one can attain a fixed position in space and record the flow of physical 'particles' along this point in order to describe motion and deformation of matter. The latter approach is normally termed the Eulerian description, and it is mainly used in fluid mechanics. This separation in approaches for solid mechanics and fluid mechanics has been carried over to the numerical applications that have emerged in more recent years.

A number of different strategies have been proposed for coupling the response of interacting solids and fluids. In the conventional Arbitrary-Lagrangian-Eulerian (ALE) approach (Donea et al., 1982), the coupling of the fixed Eulerian and moving Lagrangian meshes is accomplished through an intermediate region in which the conforming mesh moves with a prescribed velocity. The specification of the mesh evolution in the transition region is crucial to the success of ALE methods, which unfortunately requires some a priori knowledge of the solution. Alternatively, the called method Eulerian-Lagrangian (Legay et al., 2006) uses an Eulerian description for the fluid and a Lagrangian description for the structure. In contrast to ALE treatments of the fluid, no motion of the fluid mesh is needed to accommodate motions of the fluid-structure interface which is described by a level set (Sethian, 1999), i.e. by an implicit function. This simplifies the solution of problems involving large deformations of the structure and makes possible the treatment of problems with large changes in the topology where ALE methods often founder, but the interface will not be represented accurately for comparable levels of spatial discretization. Typical difficulties of these strategies include the treatment of the convective terms and the incompressibility constraint in the fluid equations, the modelling and tracking of the free surface in the fluid, the transfer of information between the fluid and solid domains via the contact interfaces, the modelling of wave splashing, the possibility to deal with large rigid body motions of the structure within the fluid domain, the efficient updating of the meshes for both the structure and the fluid, the impossibility of a monolithic treatment because the simultaneous solution of the fluid/structure is in general computationally challenging, mathematically and economically suboptimal.

In this paper, we follow the alternative way of posing the fluid as well as the structure problem in a Lagrangian framework (Idelsohn et al., 2007). This approach allows to treat the whole FSI domain, containing both fluid and solid subdomains which interact with each other, as a single entity and describes its behaviour by a single set of momentum and continuity equations. The equations are discretized with the Particle Finite Element Method (PFEM) (Idelsohn et al., 2004). The PFEM, treats the mesh nodes in the fluid and solid domains as particles which can freely move and even separate from the main fluid domain representing, for instance, the effect of water drops. A finite element mesh connects the nodes defining the discretized domain where the governing equations are solved in the standard FEM fashion.

The layout of the paper is the following: In the next section the basis of the Lagrangian and Eulerian descriptions are briefly presented. Next the constitutive equations are derived. Then the discretization of these equations in space and time is then discussed. Details of the basic ideas of the PFEM are outlined. Finally, numerical results in three dimensional problems are presented.

2 EQUATIONS OF MOTION

Neglecting thermomechanical effects, the motion of the elemental particles of any continuum material (fluid, solid or gas) can be determined by the equations of conservation of mass and momentum. These equations can be postulated as the continuum form of classical Newton's equations of motion and are independent of the material constitution or geometry. Using an Eulerian description, i.e. looking at the elemental particles as they pass through fixed positions in the physical space, the equations of conservation of mass and momentum can be stated in local form as:

$$\frac{D\rho(x, t)}{Dt} = -\rho(x, t) \operatorname{div} V(x, t) \quad (1)$$

$$\rho(x, t) \frac{DV(x, t)}{Dt} = \operatorname{div} \sigma(x, t) + \rho(x, t) \mathbf{b}(x, t) \quad (2)$$

where $\sigma(x, t)$ is the Cauchy stress, and, $\rho(x, t)$ and $V(x, t)$ are the density and the velocity vector of the elemental particles that at time t pass through the position x , respectively. $\frac{D\phi}{Dt}$ denotes the total or material time-derivative of ϕ . In the absence of couple stresses the Cauchy stress is a second order symmetric tensor. In the Eulerian description the divergence div is taken with respect to the spatial coordinates x . For example, div computed in cartesian coordinates $x = x_k e_k$ is:

$$\operatorname{div} V = \frac{\partial V_k}{\partial x_k}$$

At any time t equations (1) and (2) can be solved on the whole volume Ω_t occupied by the material body, provided one knows the external body forces \mathbf{b} (per unit of mass) and surface forces \bar{t} .

We can write equivalent conservation equations using a Lagrangian Formulation. In the Lagrangian description, one essentially follows the history of individual particles. Consequently, two independent variables are taken: the time t of evolution and a vector-type label associated to each particle. The label can be conveniently taken as the reference position vector X of the particle at some initial reference time $t = 0$. In this description, then, any quantity M is expressed as $M = M(X, t)$. In particular, the particle position is written as

$$x = \chi(X, t) \quad (3)$$

which represents the location at t of the particle whose position was X at $t = 0$.

The knowledge of the deformation map χ for all the elemental particles completely defines the motion and deformation of the material body. In particular the velocities can be computed by:

$$V(X, t) = \frac{\partial \chi(X, t)}{\partial t} = \frac{Dx}{Dt} \quad (4)$$

Assuming the existence of the deformation map it is possible to rewrite the conservation equations (1) and (2) in terms of the reference coordinates \mathbf{X} :

$$\rho(x, t) = \rho(\chi(X, t)) = \frac{\rho_0(X, t)}{J(X, t)} \quad (5)$$

$$\rho_0(X, t) \frac{DV(X, t)}{Dt} = \operatorname{Div} P(X, t) + \rho_0 f(X, t) \quad (6)$$

where $\rho_0(X, t)$ is the density of the material in the reference configuration, $J(X, t)$ is the Jacobian

$$J(X, t) = \det F(X, t) \quad (7)$$

of the deformation gradient

$$F(X, t) = \frac{\partial x}{\partial X} = \text{Grad}(\chi(X, t)) \quad (8)$$

and $P(X, t)$ is the first Piola-Kirchhoff stress tensor

$$P(X, t) = J(X, t)\sigma(\chi(X, t)) \cdot F^{-T}(X, t) \quad (9)$$

Note that the differential operators divergence and gradient are written in lower-case letters (*div*, *grad*) when computed with respect to spatial coordinates x_k and in capital letters (*Div*, *Grad*) when computed with respect to material coordinates X_k .

From now on, we simplify the notation by writing the physical quantities without referencing their explicit dependence on time and on material or spatial coordinates. Then, the conservation equations (5) and (6) can be rewritten simply as:

$$\rho = \frac{\rho_0}{J} \quad (10)$$

$$\rho_0 \frac{DV}{Dt} = \text{Div}P + \rho_0 f \quad (11)$$

with the Jacobian given by:

$$J = \det F \quad (12)$$

and the first Piola-Kirchhoff stress by:

$$P = J\sigma \cdot F^{-T} \quad (13)$$

Observe that in the Lagrangian formulation, conservation of mass (10) is a direct consequence of a straightforward computation of the density in terms of the Jacobian and of the initial density configuration ρ_0 . The momentum equation has to be solved in conjunction with the boundary conditions representing the external loads and motion restrictions under which the material body is moving. In most of the cases one specifies surface forces t at certain surfaces Γ_σ of the boundary Γ of the body and impose prescribed displacements in the remaining parts Γ_U of the material's boundary:

$$\sigma \cdot n = \bar{t} \quad \text{on} \quad \Gamma_\sigma \quad (14)$$

$$U = \bar{U} \quad \text{on} \quad \Gamma_U \quad (15)$$

Equations (10)-(15) are independent of the material, so we need to incorporate the information of the specific material we want to model. This is done by means of specifying the material's constitutive equation, which basically links the stress tensor to the deformation. In the context of the present paper we treat the problem of simulating incompressible newtonian fluids and isotropic hypoelastic solids either separately or in the form of a fluid-structure interaction. Accordingly in the next section we discuss their constitutive equations.

3 CONSTITUTIVE EQUATIONS

3.1 Constitutive Equation of Incompressible or Nearly-Incompressible Newtonian Fluids

We treat the incompressible fluid as the limit case of a nearly-incompressible newtonian flow. The constitutive equation of a newtonian fluid is a linear relationship between the Cauchy stress σ and the deformation rate tensor D :

$$\sigma = -pI - \frac{2}{3}\mu_f(trD)I + 2\mu_f D \quad (16)$$

where μ_f is the fluid viscosity and p is the thermodynamic (or hydrostatic) pressure of the fluid. By definition D is the symmetric part

$$D = \frac{1}{2}(L + L^T) \quad (17)$$

of the velocity gradient tensor:

$$L = gradV \quad (18)$$

Note that:

$$trD = divV = \varepsilon_v \quad (19)$$

If D is decomposed in its volumetric and its deviatoric components:

$$D = \left[\frac{1}{3}(trD)I + \acute{D} \right] = \left[\frac{1}{3}\varepsilon_v I + \acute{D} \right] \quad (20)$$

We can write (19) as:

$$\sigma = -pI + 2\mu_f \acute{D} \quad (21)$$

Following (Kundu and Cohen, 2002), if the newtonian flow is nearly-incompressible then density changes are related to pressure changes by the following relationship:

$$dp = \frac{K_f}{\rho} d\rho \quad (22)$$

where K_f is the elastic bulk modulus of the fluid. Then applying the material time derivative to the equation above and using the equation of conservation of mass we get:

$$\frac{Dp}{Dt} = \frac{K_f}{\rho} \frac{D\rho}{Dt} = - K_f divV \quad (23)$$

3.2 Time-Discretization of the Constitutive Equation of a Newtonian Fluid

A implicit discretization of the fluid's constitutive equation (21) is:

$$\sigma^{(n+1)} = -p^{(n+1)}I + 2\mu_f \acute{D}^{(n+1)} \quad (24)$$

The discretized version of equation (23) for nearly incompressible flows would be:

$$\frac{p^{(n+1)} - p^{(n)}}{\Delta t} = -K_f div^{(n+1)}V^{(n+1)} \quad (25)$$

So:

$$p^{(n+1)} = p^{(n)} - \Delta t K_f \varepsilon_v^{(n+1)} \quad (26)$$

replacing (26) in (24), we have:

$$\sigma^{(n+1)} = -p^{(n)}I + \Delta t K_f \varepsilon_v^{(n+1)}I + 2\mu_f \acute{D}^{(n+1)} \quad (27)$$

3.3 Constitutive Equation of Hypoelastic Solids

A isotropic hypoelastic solid (Truesdell and Noll, 1992) is a material whose constitutive equation is given by a linear isotropic relationship between the stress rate and the deformation rate:

$$\frac{\Delta}{\tau} = 2\mu_h D + \lambda_h (\text{tr} D) I \quad (28)$$

where $\frac{\Delta}{\tau}$ is the Truesdell rate

$$\frac{\Delta}{\tau} = \dot{\tau} - L \cdot \tau - \tau \cdot L^T = F \cdot \dot{S} \cdot F^T \quad (29)$$

of the Kirchhoff stress tensor $\tau = J\sigma$ and \dot{S} is the material time-derivative of the second Piola-Kirchhoff stress:

$$S = F^{-1} \cdot P = JF^{-1} \cdot \sigma \cdot F^{-T} \quad (30)$$

3.4 Time-discretization of the constitutive equation of an hypoelastic solid

A implicit discretization of the constitutive rate equation is:

$$\frac{\Delta^{(n+1)}}{\tau} = 2\mu_h D^{(n+1)} + \lambda_h (\text{tr} D^{(n+1)}) I \quad (31)$$

The Truesdell rate of the Kirchhoff stress is written within the interval as

$$\frac{\Delta^{(n+1)}}{\tau} = F^{(n+1)} \cdot \dot{S}^{(n+1)} \cdot F^{T(n+1)} \quad (32)$$

where $F^{(n+1)}$ is the deformation gradient up to time $t^{(n+1)}$. Applying the generalized mid-point rule for $\dot{S}^{(n+1)}$

$$\dot{S}^{(n+1)} = \frac{S^{(n+1)} - S^{(n)}}{\Delta t} \quad (33)$$

we get

$$F^{(n+1)} \cdot (S^{(n+1)} - S^{(n)}) \cdot F^{T(n+1)} = 2\mu \Delta t D^{(n+1)} + \lambda \Delta t (\text{tr} D^{(n+1)}) I \quad (34)$$

using that $F \cdot S \cdot F^T = J\sigma$ and the so-called incremental deformation tensor $f^{(n+1)}$ defined as:

$$f^{(n+1)} \cdot F^{(n)} = F^{(n+1)} \quad (35)$$

we get:

$$J^{(n+1)} \sigma^{(n+1)} = J^{(n)} f^{(n+1)} \cdot \sigma^{(n)} \cdot f^{T(n+1)} + \lambda_h \Delta t (\text{tr} D^{(n+1)}) I + 2\mu_h \Delta t D^{(n+1)} \quad (36)$$

The equation (36) can be applied for both formulations. However in this paper we will use the Updated Lagrangian approach (see Section 4), then it suffices to replace $f^{(n+1)}$ by $F^{(n+1)}$ and $J^{(n)}$ by 1. Defining

$$\bar{\mu}_h^{(n+1)} = \frac{\mu_h \Delta t}{J^{(n+1)}}, \bar{\lambda}_h^{(n+1)} = \frac{\lambda_h \Delta t}{J^{(n+1)}} \quad (37)$$

and the tensor

$$\hat{\sigma}_h^{(n)} = \frac{1}{J^{(n+1)}} F^{(n+1)} \cdot \sigma^{(n)} \cdot F^{T(n+1)} \quad (38)$$

we obtain the stress update expression:

$$\sigma^{(n+1)} = \hat{\sigma}_h^{(n)} + \bar{\lambda}_h^{(n+1)} (tr D^{(n+1)}) I + 2\bar{\mu}_h^{(n+1)} D^{(n+1)} \quad (39)$$

Decomposing the deformation rate tensor in terms of their deviatoric and volumetric part in the above equation, we obtain the following alternative expression:

$$\sigma^{(n+1)} = \hat{\sigma}_h^{(n)} + \left(\bar{\lambda}_h^{(n+1)} + \frac{2}{3} \bar{\mu}_h^{(n+1)} \right) (\varepsilon_v^{(n+1)}) I + 2\bar{\mu}_h^{(n+1)} \dot{D}^{(n+1)} \quad (40)$$

Defining a hypoelastic volumetric viscosity:

$$\kappa_h = \bar{\lambda}_h + \frac{2}{3} \bar{\mu}_h \quad (41)$$

We get:

$$\sigma^{(n+1)} = \hat{\sigma}_h^{(n)} + \kappa_h^{(n+1)} \varepsilon_v^{(n+1)} I + 2\bar{\mu}_h^{(n+1)} \dot{D}^{(n+1)} \quad (42)$$

This is a discrete version of the constitutive equation of an hypoelastic material.

3.5 A unique constitutive formulation for a Newtonian Fluid and a Hypoelastic Solid

Now we make use of the similarity between the constitutive equation of the hypoelastic solid (42) and the constitutive equation of a Newtonian fluid (27) so as to write a unique constitutive equation for both materials. The only differences between the constitutive equations is the fact that the Lam Coefficients for the hypoelastic solid are not longer constant. As a consequence we can write the following general expressions for both materials:

$$\sigma^{(n+1)} = \hat{\sigma}^{(n)} + \mathcal{K}^{(n+1)} \varepsilon_v^{(n+1)} I + 2\mu^{(n+1)} \dot{D}^{(n+1)} \quad (43)$$

where

$$\begin{aligned} \mu^{(n+1)} &= \begin{cases} \bar{\mu}_h = \frac{\mu_h \Delta t}{J^{(n+1)}} & \text{if Hypoelastic solid} \\ \mu_f^{(n+1)} & \text{if Newtonian fluid} \end{cases} \\ \mathcal{K} &= \begin{cases} \frac{\lambda_h \Delta t}{J^{(n+1)}} + \frac{2}{3} \frac{\mu_h \Delta t}{J^{(n+1)}} & \text{if Hypoelastic solid} \\ \Delta t K_f & \text{if Newtonian fluid} \end{cases} \\ \hat{\sigma}^{(n)} &= \begin{cases} \frac{1}{J^{(n+1)}} F^{(n+1)} \cdot \sigma^{(n)} \cdot F^{T(n+1)} & \text{if Hypoelastic solid} \\ -p^{(n)} I & \text{if Newtonian fluid} \end{cases} \end{aligned} \quad (44)$$

4 TIME-DISCRETIZATION OF EQUATIONS OF MOTION USING A LAGRANGIAN FORMULATION

To obtain numerical solutions to equations (10)-(15) we use a Lagrangian Formulation. The formulation can be made either Total Lagrangian or Updated Lagrangian. In the former the reference configuration is the initial one, in the second the reference configuration is chosen to be the most recent computed configuration and it is updated every time step. In this paper we will use the Updated Lagrangian approach only. Having chosen a reference configuration which corresponds to a volume Ω_0 with a density distribution ρ_0 , applying the Newmark method (Newmark, 1959) to integrate in the time the equations (10) and (11) leads to:

$$\rho_0 A^{(n+1)} = Div (J^{(n+1)} \sigma^{(n+1)} \cdot F^{-T(n+1)}) + \rho_0 b^{(n+1)} \quad (45)$$

with

$$\rho^{(n+1)} = \frac{1}{J^{(n+1)}} \rho_0 \quad (46)$$

where

$$U^{(n+1)} = U^{(n)} + \Delta t V^{(n)} + \Delta t^2 \left(\left(\frac{1}{2} - \beta \right) A^{(n)} + \beta A^{(n+1)} \right) \quad (47)$$

$$V^{(n+1)} = V^{(n)} + \Delta t \left((1 - \gamma) A^{(n)} + \gamma A^{(n+1)} \right) \quad (48)$$

The values of γ and β are 0.5 and 0.25 respectively. The above equations are solved in the reference volume Ω_0 and the boundary conditions imposed on the reference volume's boundary $\Gamma_0 = \Gamma_{0U} + \Gamma_{0\sigma}$.

Equations (10)-(15) or their discrete form (45)-(46) are independent of the material, so we need to incorporate the materials constitutive equations. In the context of the present paper we treat the problem of simulating quasi-incompressible newtonian fluids and isotropic hypoelastic solids either separately or in the form of a fluid-structure interaction.

5 INTEGRATION OF MOTION EQUATIONS

Inserting the general constitutive equation (43) into equation (45) and assuming an Updated Lagrangian Approach (i.e. $\rho_0 = \rho^{(n)}$) we get:

$$2\rho^{(n)} \left(\frac{V^{(n+1)} - V^{(n)}}{\Delta t} \right) = \rho^{(n)} \frac{A^{(n)}}{\Delta t} + Div (J^{(n+1)} \hat{\sigma}^{(n)} \cdot F^{-T(n+1)}) + Div (J^{(n+1)} \mathcal{K}^{(n+1)} \varepsilon_v^{(n+1)} I \cdot F^{-T(n+1)}) + Div (J^{(n+1)} 2\mu^{(n+1)} \acute{D}^{(n+1)} \cdot F^{-T(n+1)}) + \rho^{(n)} b^{(n+1)} \quad (49)$$

Now in order to ease readiness, we will drop the upper-index $(n + 1)$ from the unknown quantities. So for example $F^{-T(n+1)}$ will be written simply as F^{-T} . Note that we keep the index (n) of the known quantities. Using this convention we can rewrite the above equation as:

$$2\rho^{(n)} \left(\frac{V - V^{(n)}}{\Delta t} \right) = \rho^{(n)} \frac{A^{(n)}}{\Delta t} + Div (J \hat{\sigma}^{(n)} \cdot F^{-T}) + Div (JK \varepsilon_v I \cdot F^{-T}) + Div (J 2\mu \acute{D} \cdot F^{-T}) + \rho^{(n)} b \quad (50)$$

5.1 Spatial Discretization

Multiplying equation (50) by the test function W and (23) by q and integrating over the domain, we arrive at :

$$\int_{\Omega_n} 2\rho^{(n)}W \cdot \left(\frac{V - V^{(n)}}{\Delta t} \right) dV_n = \int_{\Omega_n} W \cdot \left(\rho^{(n)} \frac{A^{(n)}}{\Delta t} + Div (J\hat{\sigma}^{(n)} \cdot F^{-T}) + Div \left(J \left(\mathcal{K} - \frac{2}{3}\mu \right) \varepsilon_v I \cdot F^{-T} \right) \right) + \int_{\Omega_n} W \cdot (Div (J\mu (gradV + grad^T V) \cdot F^{-T}) + \rho^{(n)}b) dV_n + \int_{\Gamma_n} W(T - P \cdot N) d\Gamma_n \quad (51)$$

$$\int_{\Omega_n} qp^{(n+1)} dV_n = \int_{\Omega_n} q(\hat{p}^{(n+1)} - \mathcal{K}\varepsilon_v^{(n+1)}) dV_n \quad (52)$$

After integration by parts, equation (51) becomes:

$$\int_{\Omega_n} 2\rho^{(n)}W \cdot \left(\frac{V - V^{(n)}}{\Delta t} \right) dV_n = \int_{\Omega_n} W \cdot \rho^{(n)} \frac{A^{(n)}}{\Delta t} dV_n - \int_{\Omega_n} GradW : (J\hat{\sigma}^{(n)} \cdot F^{-T}) dV_n - \int_{\Omega_n} GradW : \left(J \left(\mathcal{K} - \frac{2}{3}\mu \right) \varepsilon_v I \cdot F^{-T} \right) dV_n - \int_{\Omega_n} GradW : (J\mu (GradV + Grad^T V) \cdot F^{-1} \cdot F^{-T}) dV_n + \int_{\Omega_n} \rho^{(n)}W \cdot b dV_n + \int_{\Gamma_n} W \cdot T d\Gamma_n \quad (53)$$

The velocity and the pressure are approximated as:

$$\begin{aligned} V_j &= \sum W_i(X, t) V_{i,j} \\ p &= \sum W_i(X, t) P_i \end{aligned} \quad (54)$$

where W_i are the MFEM shape functions and V and p the nodal values of the three components of the unknown velocity and the pressure respectively. More details of the mesh discretization process and the choice of shape functions are given in section 8. Substituting the approximation (54) into (52)-(53) and choosing a Galerkin method leads to the following systems of equations:

$$(2M + \Delta tK) V = 2MV^{(n)} + MA^{(n)} - \Delta tD\hat{\sigma}^{(n)} + \Delta tF \quad (55)$$

$$\widehat{M}p = \widehat{M}p^{(n)} - GV \quad (56)$$

where the previous matrices are:

$$\begin{aligned}
M_{ij} &= \int_{\Omega_n} \rho^{(n)} W_i W_j dV_n \\
\widehat{M}_{ij} &= \int_{\Omega_n} W_i W_j dV_n \\
K_{ij} &= \int_{\Omega_n} \text{Grad} W_i F^{-1} \mu (\text{Grad} W_j + \text{Grad}^T W_j) F^{-1} J dV_n + \\
&\quad \int_{\Omega_n} \text{Grad} W_i F^{-T} \left(\mathcal{K} - \frac{2}{3} \mu \right) \text{Grad} W_j F^{-T} J dV_n
\end{aligned} \tag{57}$$

$$\begin{aligned}
D_{ij} &= \int_{\Omega_n} \text{Grad} W_i W_j F^{-T} J dV_n \\
G_{ij} &= \int_{\Omega_n} W_i \mathcal{K} \text{Grad} W_j F^{-T} dV_n \\
F_i &= \int_{\Omega_n} W_i b dV_n + \int_{\Gamma_n} W_i T d\Gamma_n
\end{aligned} \tag{58}$$

6 SUMMARY OF A FULL ITERATIVE TIME STEP

The resulting nonlinear system of equations (55)-(56) has to be solved iteratively. Therefore, a Picard iteration is used for the linearization of all equations, leading to a relatively simple fixed point type solution procedure. A full time step may be described as follows: starting with the known values $X^{(n)}, V^{(n)}$ and $\sigma^{(n)}$ in each particle, the computation of the new particle position involve the following steps:

- 1- Initialize $F^{(n+1,0)} = \delta_{ij} e_i \otimes e_j, J^{(n+1,0)} = 1, x^{(n+1,0)} = X^{(n)}$
- 2- While (not converge)

(a) Evaluate the velocity $V^{(n+1,i+1)}$

$$(2M + \Delta t K) V^{(n+1,i+1)} = 2M V^{(n)} + M A^{(n)} - \Delta t D \widehat{\sigma}^{(n)} + \Delta t F^{(n+1)} \tag{60}$$

(b) Move the particles to the $x^{(n+1,i+1)}$ position with

$$x^{(n+1,i+1)} = X^{(n)} + U^{(n+1,i+1)} \tag{61}$$

(c) Compute the deformation gradient $F^{(n+1,i+1)}$ from (8) and $J^{(n+1,i+1)}$ from (7)

3- If converge

(a) Evaluate the pressure $p^{(n+1)}$ only for the fluid domain

$$\widehat{M} p^{(n+1)} = \widehat{M} p^{(n)} - G V^{(n+1)} \tag{62}$$

(b) Evaluate the $\sigma^{(n)}$ only for the solid domain

$$\sigma^{(n+1)} = \widehat{\sigma}^{(n)} + \mathcal{K}^{(n+1)} \varepsilon_v^{(n+1)} I + 2\mu^{(n+1)} \dot{D}^{(n+1)} \tag{63}$$

(c) update the mesh nodes with

$$X^{(n+1)} = x^{(n+1,i+1)} \quad (64)$$

5-Generate the new mesh

6-Compute the new time step

7 THE BASIS OF THE PARTICLE FINITE ELEMENT METHOD

Let us consider a domain containing both fluid and solid subdomains. The moving fluid particles interact with the solid boundaries thereby inducing the deformation of the solid which in turn affects the flow motion and, therefore, the problem is fully coupled. The finite element method (FEM) is used to solve the continuum equations in both domains. Hence a mesh discretizing these domains must be generated in order to solve the governing equations for both the fluid and solid problems in the standard FEM fashion. We note again that the nodes discretizing the fluid and the solid domains are viewed as material particles which motion is tracked during the transient solution. This is useful to model the separation of fluid particles from the main fluid domain and to follow their subsequent motion as individual with a known density, an initial acceleration and velocity and subject to gravity forces. The quality of the numerical solution depends on the discretization chosen as in the standard FEM. Adaptive mesh refinement techniques can be used to improve the solution in zones where large motions of the fluid or the structure occur.

8 MESH GENERATION

A key point for the success of the Lagrangian FSI formulation is the fast regeneration of a mesh at every time step on the basis of the position of the nodes in the space domain. The mesh is generated using the so called extended Delaunay tessellation (EDT) presented in (Idelsohn et al., 2003; Edelsbrunner and Mucke, 1999). The C^0 continuous shape functions of the elements can be simply obtained using the so called meshless finite element interpolation (MFEM). Details of the mesh generation procedure and derivation of the MFEM shape functions can be found in (Idelsohn et al., 2003; Edelsbrunner and Mucke, 1999). One of the main problems in mesh generation is the correct definition of the boundary domain. The use of the extended Delaunay partition makes it easier to recognize boundary nodes.

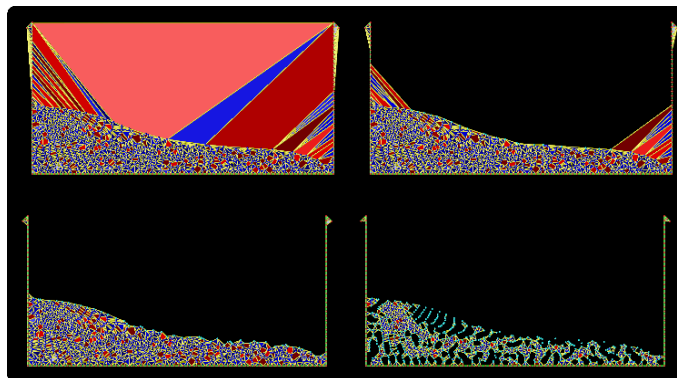


Figure 1: Alpha Shape of the cloud of points ($\alpha = 100, 10, 1, 0.7$)

Considering that the particles follow a variable $h(x)$ distribution, where $h(x)$ is the minimum distance between two particles, the following criterion has been used: All particles on an empty sphere with a radius $r(x)$ bigger than $h(x)$, are considered as boundary nodes. α is a parameter close to, but greater than one. Note that this criterion is coincident with the Alpha Shape concept (Edelsbrunner and Mucke, 1999). Figure 1 shows an example of the boundary recognition using the Alpha Shape technique.

In this work, the boundary surface is defined by all the polyhedral surfaces (or polygons in 2D) having all their nodes on the boundary and belonging to just one polyhedron.

The method described also allows one to identify isolated fluid particles outside the main fluid domain.

9 EXAMPLES

9.1 Collapse of a water column

The collapse of a water column is calculated using the present formulation and results compared with experiment results obtained by S. Koshizuka in reference (Koshizuka et al., 1995). Geometry of the initial water column is illustrated in Figure 2. The fluid properties correspond to water, so that $\rho = 1000[kg/m^3]$ and $\mu = 0.001[kg/sm]$. The system is simulated for $1[s]$ with a time steps = $0.0025[s]$. Figure 3 show the experimental and the numerical results at different characteristic time step. The results compare considerably well with the experimental results.

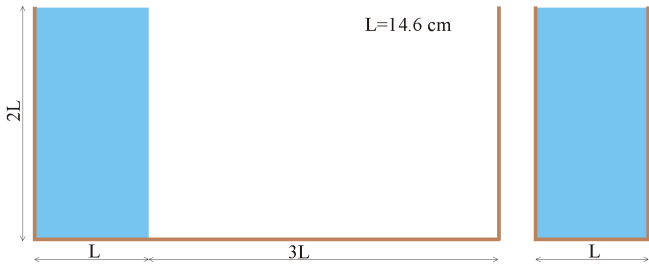


Figure 2: Initial geometry of the water column (side view and front view)

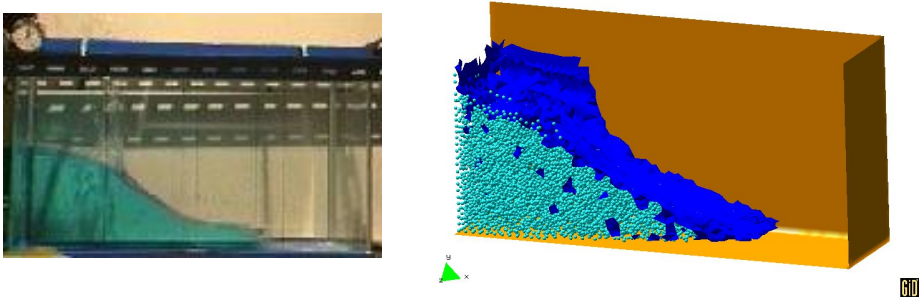
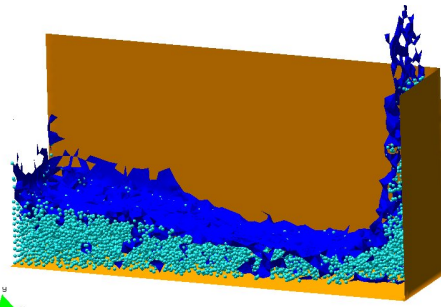
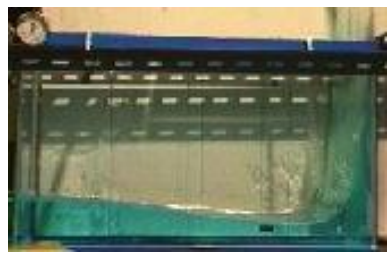
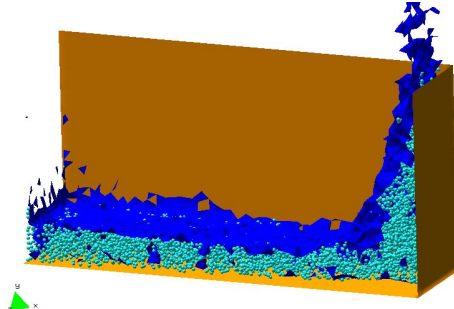


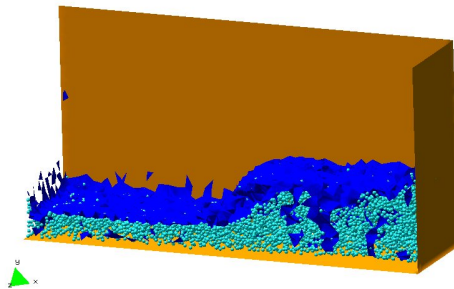
Figure 3: Collapsing water column for t=0.2



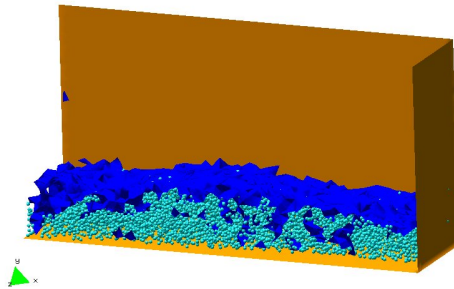
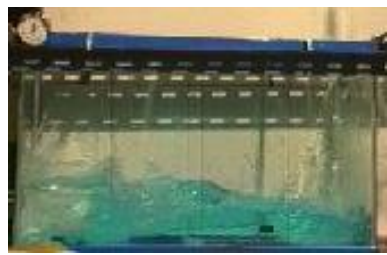
0.4



0.6



0.8



1.0

Figure 4: (continued) $t=0.4, 0.6, 0.8, 1$

9.2 Collapse of a water with a circular cylinder

The problem of a broken dam over a circular cylinder is of practical importance in terms of functional and structural design of hydraulic structures. The material parameters are given by the density $\rho = 2500[kg/m^3]$, the Youngs modulus $E = 10^6[kg/s^2m]$ and the Poissons ratio $\nu = 0.3$. The cylinder has a radius $r = 1.5[cm]$ and a height of $h = 15[cm]$.

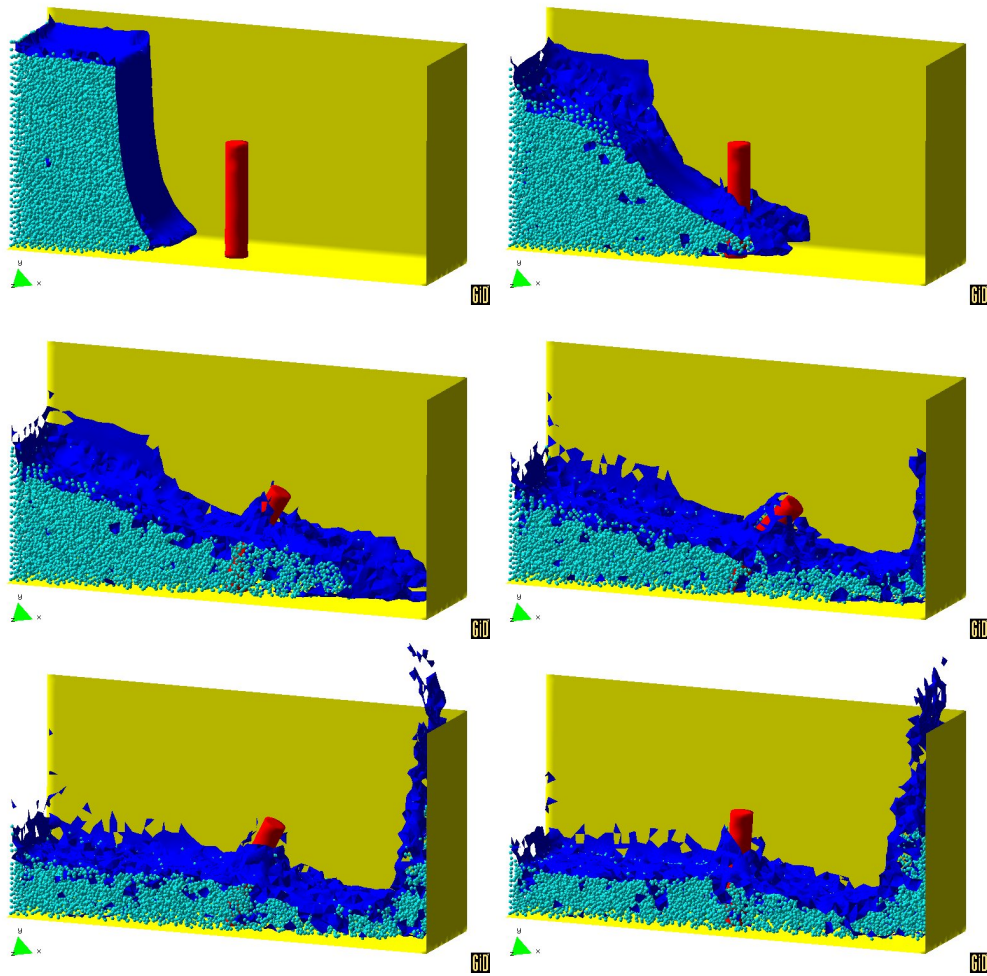


Figure 5: Collapsing water column with obstacle $t=0.1, 0.19, 0.28, 0.36, 0.46, 0.53$

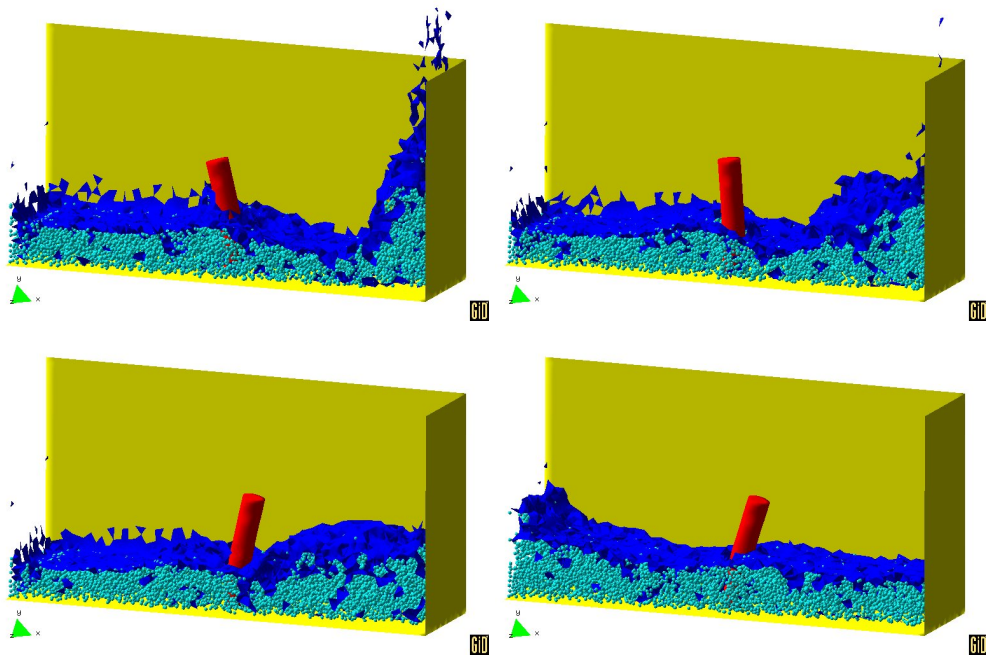


Figure 6: (continued) $t=0.6, 0.7, 0.76, 0.93$

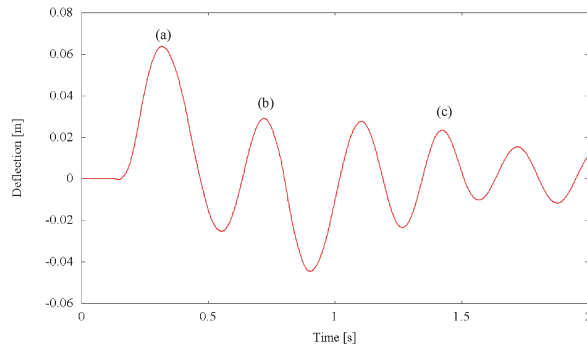


Figure 7: History of the displacement

No experimental results have been found for this example, but the shape of the deformation of the cylinder as well as the free surface perturbation seems to be in agreement with the physics of the problem. Figure 5 shows a time sequence of the free surface elevation. The left upper corner of the cylinder first gets a deflection to the left when the water acts on the its lower parts and moves to the right while the water is running on the bottom wall. It obtains its maximum deflection (mark (a) in Figure 7). While the water goes up losing its momentum, the cylinder moves to the left. Finally, when the water falls down into the remaining water, a new reflected wave flies toward the left and the impact of the fluid causes the cylinder to start oscillating (b). This oscillation is damped (c) by the reflected waves. The horizontal force acting on the cylinder is showed in Figure 8.

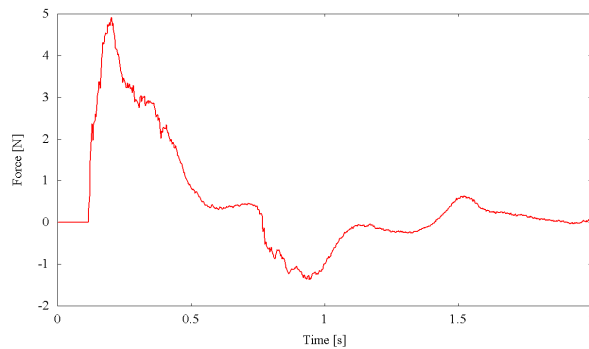


Figure 8: The force acting on the circular cylinder

10 CONCLUSIONS

In this paper, the Particle Finite Element Method applied to solve Fluid-Structure Interaction problems in a monolithic numerical scheme was presented. The method takes advantage of the similarity between the discrete constitutive equations of the materials under consideration: quasi-incompressible newtonian fluid and hypoelastic solid, and it has proved to be ideal to treat problems involving fluid with free surfaces and structures which can undergo large structural displacements, rotations and deformations. Other, essential solution ingredients of the numerical approach are: the Delaunay triangulation algorithm which provides a very efficient connectivity scheme, and, the identification of boundary nodes using an Alpha-Shape type technique. The examples presented have shown the great potential of the PFEM for solving a wide class of practical FSI problems.

11 ACKNOWLEDGEMENTS

The authors thank Dr. R. Rossi and Mr. M. A. Celigueta for many useful discussions. This work was supported by the Programme $\text{Al}\beta\text{an}$, the European Union Programme of High Level Scholarships for Latin America, scholarship No.E06D100984AR.

REFERENCES

- Donea J., Guiliani S., and Halleux J. An arbitrary lagrangian-eulerian finite element method for transient fluid-structure interactions. *Computer Method in Applied Mechanics and Engineering*, 33:689–723, 1982.
- Edelsbrunner H. and Mucke E. Three dimensional alpha shapes. *ACM Trans. Graphics*, 13:43–72, 1999.
- Idelsohn S., Calvo N., and Oñate E. Polyhedrization of an arbitrary point set. *Computer Method in Applied Mechanics and Engineering*, 192:2648–2668, 2003.
- Idelsohn S., Marti J., Limache A., and Oñate E. Unified lagrangian formulation for elastic solids and incompressible fluids. application to fluid-structure interaction via the pfem. *Computer Method in Applied Mechanics and Engineering*, 2007.
- Idelsohn S., Oñate E., and Del Pin F. The particle finite element method: a powerful tool to solve incompressible flows with free-surfaces and breaking waves. *International Journal for Numerical Methods in Engineering*, 61:(7)964–989, 2004.
- Koshizuka S., Tamko H., and Oka Y. A particle method for incompressible viscous flow with fluid fragmentation. *International Journal of Computational Fluid Dynamics*, 1:29–46, 1995.

- Kundu P. and Cohen I. *Fluid Mechanics*. Academic Press, 2002.
- Legay A., Chessa J., and Belytschko T. An eulerian-lagrangian method for fluid-structure interaction based on level sets. *Computer Method in Applied Mechanics and Engineering*, 195:2070–2087, 2006.
- Newmark N. A method of computation for structural dynamics. *Proc. A.S.C.E.*, 8:67–94, 1959.
- Sethian J. *Level set methods and fast marching methods evolving interfaces in computational geometry*. fluid mechanics, computer vision and materials science, Cambridge University, 1999.
- Truesdell C. and Noll W. The non-linear field theories of mechanics. *Handbuch der Physik, Springer, Berlin*, Bd III/3, 1992.